

Hydrogen permeation in pipeline steels

E. Fallahmohammadi, F. Bolzoni, M. V. Diamanti, L. Lazzari

Politecnico di Milano. Dipartimento di Chimica, Materiali ed Ingegneria Chimica “Giulio Natta” Via Mancinelli, 7, Milano 20131, Italy.

ABSTRACT

The electrochemical permeation technique to study the entry, transport and trapping of hydrogen in metals is outlined. This paper deals with diffusion and trapping mechanisms of hydrogen to better understand the charging phenomenon and the hydrogen distribution in carbon (API 5L X65) and a low alloy steel (ASTM A182 F22) by means of the electrochemical method developed by Devanathan and Stachurski. Moreover Ferritic perlite steel material namely API 5L grade B, not specifically produced for sour service was considered for comparison. The lattice diffusivity of hydrogen was found by means of partial permeation transient.

Keywords: Hydrogen permeation, trapping, lattice diffusion

1 INTRODUCTION

In a previous phase of this research, an electrochemical method setup to charge large specimens with hydrogen was illustrated. Mechanical tests carried out on specimens charged with hydrogen proved that hydrogen significantly affected the fracture toughness of the tested carbon or low alloy steels, as fracture mechanics tests demonstrated [1, 2]. To interpret the results, an improved knowledge of the kinetics of hydrogen adsorption, entry and transport process in steel is required. In general, one may distinguish the following processes in a metal/hydrogen system: (i) the entry of hydrogen from the surrounding environment into the metal, (ii) the transport (diffusion) of hydrogen inside the metal and (iii) the trapping of hydrogen at structural defects [3-5]. The electrochemical permeation test procedure applied to a metallic membrane is the proper technique to characterise the hydrogen-metal system through the hydrogen flux measurement. The obtained curve dispenses quantitative information: the steady-state permeation rate, the apparent diffusion coefficient D_{app} and the apparent subsurface concentration C_{0app} . However to access the lattice diffusion coefficient and the average concentration in the membrane, hard hypothesis is generally imposed to interpret experimental data. Moreover the hydrogen trapped into the microstructure alters the evaluation of the diffusion coefficient. In order to increase our knowledge of the interactions of hydrogen with steels and better understand the charging phenomenon and hydrogen distribution in steel pipeline

material, the purpose of this research is to characterize diffusion and trapping mechanisms of hydrogen.

2 EXPERIMENTAL

Tests have been carried out on samples taken from seamless pipe in quenched and tempered conditions. Heavy wall micro-alloyed C - Mn steel, API 5L X65 and low alloy 2 ¼ Cr 1Mo steel, namely ASTM A 182 F22 which are provided for sour service applications were chosen. Microstructure of X65 steel is equiaxed and acicular ferrite with finely dispersed carbides. Microstructure of F22 samples is typical of tempered lath martensite, i.e., elongated ferrite grains with finely dispersed carbides. For both steels the microstructure is rather homogeneous neither central segregations nor elongated inclusions, which deeply influence hydrogen permeation, were present in the microstructure. Moreover Ferritic perlite steel material, namely API 5L grade B, not specifically produced for sour service was considered for comparison.

Table 1-Chemical composition of materials used

Steel	C	Si	Mn	S	P	Cr	Mo	Ni	Nb	V	Ti	Al
X65	0.11	0.28	1.18	0.007	0.017	0.17	0.15	0.42	0.02	<0.06	<0.01	0.03
F22	0.14	0.11	0.43	0.001	0.003	2.25	1.04	0.08	0.02	<0.01	<0.01	0.04
Gr B	0.18	0.25	0.7	0.003	0.025	0.11	0.01	0.03	0.03	<0.02	<0.03	0.02

Permeation experiments were carried out with the Devanathan and Stachurski [6] double cell with some modifications. Flat specimens (average thickness \approx 1 and 2 mm) were placed in an apparatus and permeation experiments were performed in their central part. The input side was in contact with a 0.4 mol L⁻¹ of CH₃COOH plus 0.2 mol L⁻¹ of CH₃COONa (pH=4.2), during the entire permeation test charging solution was de-aerated with pure nitrogen and circulated by a peristaltic pump from a 5L reservoir (flow \approx 10 L h⁻¹, velocity at the probe tip \approx 0.4 m s⁻¹). The cathodic side of the specimen was galvanostatically polarized at a constant charging current density of 0.5 mA cm⁻², where a double junction Ag/AgCl/3 mol L⁻¹ KCl// (E = 0.199 V vs. SHE at 20°C) reference electrode and Pt wire with 1.5 cm² as counter electrode were utilized. A double junction Hg/HgO/3 mol L⁻¹ NaOH// (E = -0.08 V vs. Ag/AgCl at 20°C) reference electrode suitable for alkaline environment, was utilised as a reference electrode in anodic compartment. In order to

keep constant the boundary conditions on the anodic side of the membrane and eliminating the background current from hydrogen permeation current, samples were pre-passivated before charging. The following procedure was adopted for pre-passivation of samples: i) immersion for 1h in 0.2 mol L⁻¹ NaOH solution with 65±2°C; ii) Anodic polarization with 100 mV vs. Ag/AgCl in 0.2 mol L⁻¹ NaOH solution before charging until reaching as lowest as possible current density (<0.1 μA cm⁻² on the anodic side). The potential was fixed on the anodic side (output side) at a value (+100 mV vs. Ag/AgCl) sufficient to oxidize hydrogen atoms quasi-instantly. The output flux was deduced from the measurement of the output intensity.

Two series of experiments were performed. In the first one, two successive permeations with the same cathodic current density of 0.5 mA cm⁻² were conducted with intermediate hydrogen discharge in which current was interrupted and anodic desorption current was continuously measured. In the second series permeation was first performed; when the stationary state of this permeation was reached cathodic charging current was simply increased (from 0.5 to 1 mA cm⁻²).

Figures 1 and 2 show typical permeation curves (anodic current as a function of time) obtained in the two series of experiments. In the first series (Fig. 1) after having an imposed of cathodic current, the current increases during the first permeation, reaches a stationary value, then after complete desorption and reaching passivity current increases again during the second permeation and reaches a second stationary value. In the second series (Fig. 2) the flux increases up to stationary value, then starts increasing somewhat after increasing charging current (portion AB of the curve) and reaches a new stationary value.

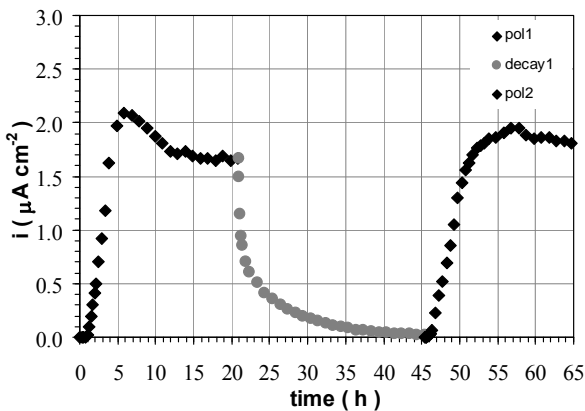


Figure 1-Typical permeation curve obtained for two successive charging with intermediate hydrogen discharge

3 DIFFUSION COEFFICIENTS

3.1 Diffusion Coefficient at the beginning of the permeation

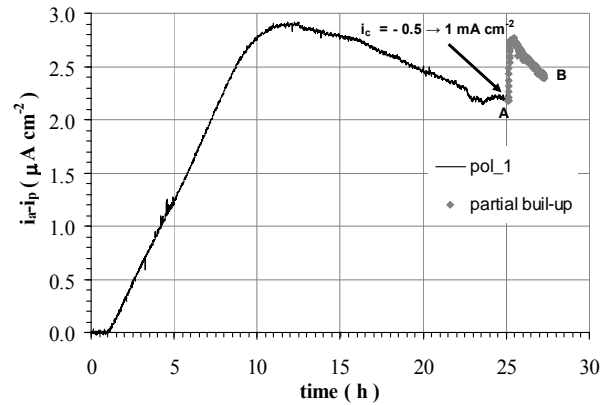


Figure 2-Typical permeation curve obtained for the second series of experiment for F22 steel (namely partial build-up: AB); cathodic current was changed from 0.5 to 1 mA cm⁻²

As mentioned in [7], in the most general case, the apparent diffusion coefficient decreases or keeps constant along the permeation curve, which means that trapping effects are minimal at the beginning of permeation. It is therefore interesting to study short time diffusion coefficients so as to eliminate trapping effects as far as possible. They are obtained by the following procedure: for a diffusion obeying Fick's usual 2nd law, in the case that the hydrogen subsurface concentration is supposed to be constant beneath the entry side $C=C_0$ and equal to zero $C=0$ at exit side, the diffusible process can be given by Fourier (or Laplace) transformation:

$$\frac{j}{j_\infty} = 1 + 2 \sum_{n=1}^{\infty} \{(-1)^n \exp(-n^2 \pi^2 \tau)\} \quad (\text{Fourier}) \quad (1)$$

$$\frac{j}{j_\infty} = \frac{2}{\sqrt{(\pi\tau)}} \sum_{n=0}^{\infty} \exp\left\{-\frac{(2n+1)^2}{4\tau}\right\} \quad (\text{Laplace}) \quad (2)$$

Where j_∞ is the hydrogen flux at steady state, as a function of the dimensionless time parameters, $\tau = Dt / L^2$ where L is the membrane thickness.

One has $\tau = 0.04$ (1% of j_∞) or by the tangent of the linear portion of the initial rising current transient $\tau = 0.05$; we compute therefore the diffusion coefficient at the beginning of permeation by the following formula

$$D(\text{beg. of perm.}) = 0.04 \text{ (or } 0.05) \frac{L^2}{t} \quad (3)$$

Table 2 shows the results obtained for the first series of experiments for three different samples. Second permeations can be observed to yield very generally identical respect to first permeations. The classical explanation of this phenomenon is that irreversible traps intervene only during the first permeation because they are saturated afterwards. In fact the difference is rather small and is negligible which means that the effect of

irreversible traps at the beginning of first permeation, i.e., the kinetics of irreversible trapping, is relatively slow as compared to diffusion. It is worthy to note that a surface effect seems to be present which may lead to affect apparent diffusivity, through the change of the potential on the entry face of the samples during galvanostatic polarisation. However at the beginning of the test potential variation is lower than end of the test. Comparing the results obtained at the beginning of the permeation for three type of samples show that apparent diffusion coefficient is one order of magnitude higher for Gr B respect to X65 and F22 steel samples; this indicates that diffusion of hydrogen in ferritic perlitic microstructure is much higher than in ferritic one (acicular ferrite (X65) or tempered lath martensite (F22)) as it is given in table 2.

Table 2-Apparent diffusion coefficient at the beginning of permeation (first series of experiments)

Material (1&2 mm)	Charge	D_{app} (average) 1% i_e ($m^2 s^{-1}$)	D_{app} (average) 3.55% i_e ($m^2 s^{-1}$)
X65	1 st	$1.68 \cdot 10^{-11}$	$1.60 \cdot 10^{-11}$
	2 nd	$1.80 \cdot 10^{-11}$	$1.70 \cdot 10^{-11}$
F22	1 st	$1.83 \cdot 10^{-11}$	$1.65 \cdot 10^{-11}$
	2 nd	$1.87 \cdot 10^{-11}$	$1.53 \cdot 10^{-11}$
Gr B	1 st	$1.16 \cdot 10^{-10}$	$1.07 \cdot 10^{-10}$
	2 nd	$1.15 \cdot 10^{-10}$	$9.20 \cdot 10^{-11}$

3.2 Diffusion coefficient at $j/j_\infty = 0.1$ and $j/j_\infty = 0.63$

These long-time coefficients are obtained in the following way: For a “normal” (Fick’s) diffusion one has $\tau = 0.066$ (10% of j_∞) and/or $\tau = 0.17$ (63% of j_∞); therefore we compute $D_{10\%}$ and $D_{63\%}$ by the formula

$$D(\text{long-time}) = 0.066 \text{ (or } 0.17) \frac{L^2}{t} \quad (4)$$

The $D_{(\text{long-time})}$ values, table 3, obtained for all materials for 1st and 2nd transients (first series of experiments) are lower than those at the beginning of permeation. As

mentioned in [7] If one starts from the quick equilibrium between lattice and reversible sites, considering increasing value of τ , one first meets a curve where the coefficient $D(t)$ decreases continuously, from $D(t)$ at the beginning to $D(t) \sim D = D_L / (1 + p_2\tau_2/\tau_1)$ at the end where $p_2\tau_2/\tau_1$ (= ratio of equilibrium total quantities of trapped and diffusible hydrogen. If one further increases τ , a rather odd behaviour occurs: j/j_∞ ratio increases first quickly, then much more slowly (slowly enough to give a “plateau”-type trend), which causes curve crossing.

Table 3-Apparent diffusion coefficient for long – time (first series of experiments)

Material (1&2 mm)	Charge	D_{app} (average) 10% i_e ($m^2 s^{-1}$)	D_{app} (average) 63% i_e ($m^2 s^{-1}$)
X65	1 st	$1.40 \cdot 10^{-11}$	$1.51 \cdot 10^{-11}$
	2 nd	$1.20 \cdot 10^{-11}$	$1.00 \cdot 10^{-11}$
F22	1 st	$1.54 \cdot 10^{-11}$	$1.43 \cdot 10^{-11}$
	2 nd	$1.45 \cdot 10^{-11}$	$1.31 \cdot 10^{-11}$
Gr B	1 st	$5.22 \cdot 10^{-11}$	$1.96 \cdot 10^{-11}$
	2 nd	$6.30 \cdot 10^{-11}$	$5.20 \cdot 10^{-11}$

That “quick-then-slow” behaviour was found by Iino [8] for irreversible (saturable) traps. No evidence of such an odd behaviour that bowing down the permeation transients or double plateau in an extreme condition that could be interpreted as the effect of irreversible traps in the case of both X65 and F22 steel samples at 20°C was observed while in the case of Gr B steel sample, not only apparent diffusivity is one order of magnitude higher at the beginning of the test but it decreases much more strongly along the curve for long-time. Moreover permeation transient starts almost immediately then much slowly and then reaches a new steady state, which is so called “double plateau” as it is shown in Fig 4. Comparison of Table 2 and 3 shows that first permeations generally yield lower D values at long-time ($j/j_\infty = 10\%$ and 63%) than at the beginning of permeation.

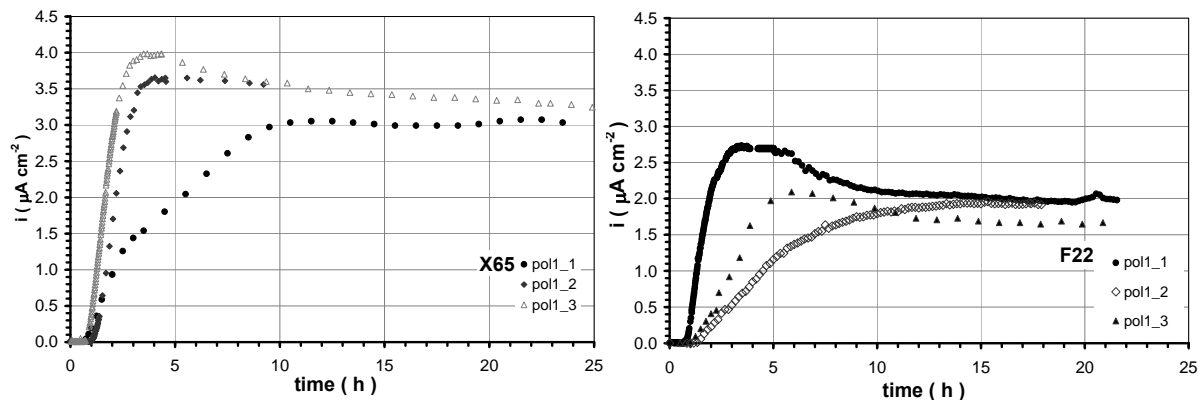


Figure 3-First permeation build-up transients A: X65; B: F22 (first series of experiments)

Results show that this type of deviation with respect to the “normal” (Fick’s) curve is compatible with the existence of irreversible trap (the deviation cannot be due to reversible traps which are in equilibrium with diffusion sites) whose filling is not very quick as compared to diffusion.

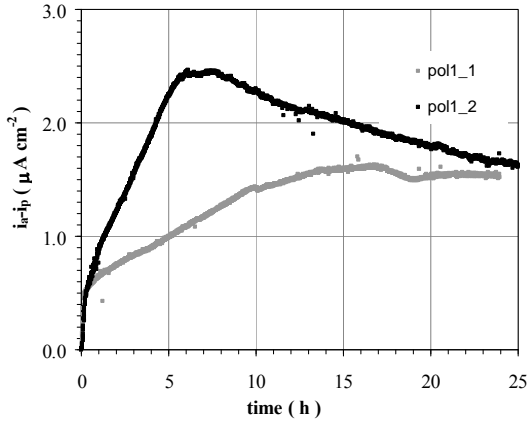


Figure 4–First permeation transient build-up for Gr B steel sample (first series of experiments)

3.3 Lattice diffusion coefficient

In second series of experiment cathodic current was increased from 0.5 to 1 mA cm⁻² after that maximum hydrogen permeation current was reached. A quite different picture was observed when the experimental and computed curves, Eq 1, matched. This suggests that when the cathodic current was increased, the hydrogen subsurface concentration C_0 immediately changed to a new constant value and transport of hydrogen controlled by the real diffusion of hydrogen into the metal. Hence, this value could be considered as hydrogen lattice diffusion coefficient, which was of the order of $1 - 4 \times 10^{-10} \text{ m}^2 \text{ s}^{-1}$ for F22 and X65.

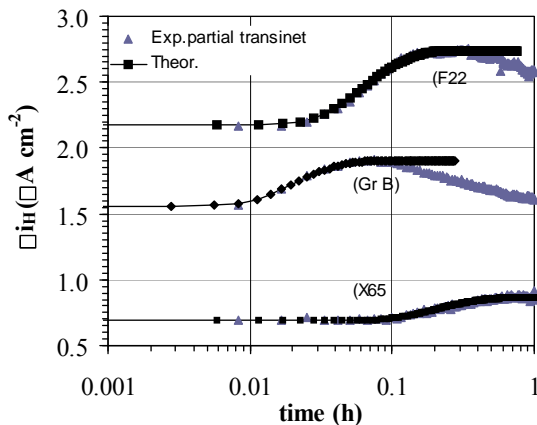


Figure 5–Partial permeation transient with increasing charging current density, 0.5 to 1 mA cm⁻² after first steady state condition. Experimental and theoretical curves are overlapped. $D_{F22} = 4 \times 10^{-10}$; $D_{X65} = 1 \times 10^{-10}$; $D_{Gr B} = 3.5 \times 10^{-9} \text{ m}^2 \text{ s}^{-1}$ (second series of experiments)

This value for Gr B sample is in the range of $3.5 \times 10^{-9} \text{ m}^2 \text{ s}^{-1}$. It seems in these cases lattice diffusivity of hydrogen was reached and it is one order of magnitude higher than hydrogen apparent diffusion coefficient.

It is worthy to note that the same behaviour was observed during potentiostatic charging as well. In such a case, the same diffusion coefficient was found from “partial transient” for the pre-charged samples. Diffusion coefficient computed from the first permeation transient and from partial transients was in the range of those ones obtained by galvanostatic charging. Partial build-up permeation transient, where $i_{p,L}$ is the permeation current and L is the thickness, is given as:

$$i_{p,L} = i_p^0 + \frac{2L(i_p^\infty - i_p^0)}{\sqrt{\pi Dt}} \sum_{n=0}^{\infty} \exp\left(-\frac{(2n+1)^2 L^2}{4Dt}\right) \quad (4)$$

Conclusion

Diffusion and trapping of hydrogen have been studied through F22 and X65 steel materials that have been considered in the previous phase of this research [1, 2] and their hydrogen diffusion coefficient compared with not specified sour service material. Apparent hydrogen diffusion coefficient and lattice diffusion coefficient for both steel samples were in the range of $1.5 \times 10^{-11} \text{ m}^2 \text{ s}^{-1}$ and $3 \times 10^{-10} \text{ m}^2 \text{ s}^{-1}$ respectively while values were one order of magnitude higher for API 5L Gr B. For both X65 and F22, no evidence of irreversible traps that mainly affect the permeation at room temperature was observed. Irreversible traps probably control the transport of hydrogen through Gr B steel samples. An analysis of the partial build-up transient for both steel samples enables to calculate the lattice diffusivity.

REFERENCES

- [1] P. Fassina, R. Morana, L. Alleva, G. Mortali, L. Vergani, A. Sciuca, proc. of Eurocorr, Moscow. (2010).
- [2] P. Fassina, F. Bolzoni, G. Fumagalli, L. Lazzari, L. Vergani, A. Sciuccati. Procedia engin. 10, pp 3226-3234, (2011).
- [3] A. Turnbull. “Hydrogen transport and cracking in metals”, Teddington, UK. pp. 129, (1994).
- [4] A. Turnbull, M. Saenz De Santa Maria, N. D. Thomas. Corrosion science, 29, pp. 89-104. (1989).
- [5] T. Zakroczymski, Electrochemical Acta. 51, pp. 2261-2266, (2006).
- [6] M. A. V. Devanathan, Z. Stachurski, Proc. Roy. Soc. A. 270, pp. 90, (1962).
- [7] E. Fallahmohammadi, F. Bolzoni, G. Fumagalli, G. Re. L. Lazzari, in course of publication, (2012).
- [8] M. Iino, Acta. metall. 30, pp. 377, (1982).